Underwater to above water LoRa transmission: technical issues and preliminary tests

Irene Cappelli, Ada Fort, Marco Mugnaini, Stefano Parrino, Alessandro Pozzebon

*Department of Information Engineering and Mathematics,
University of Siena, Via Roma 56, 53100 Siena, Italy
cappelli@diism.unisi.it, ada@diism.unisi.it, mugnaini@dii.unisi.it,
parrino2@unisi.it, alessandro.pozzebon@unisi.it*

Abstract – **The aim of this paper is to discuss the usability of Long Range (LoRa) communication technology for the transmission of data collected under fresh water to a Gateway positioned outside water. The technical feasibility of the LoRa transmission channel is discussed from a theoretical point of view, focusing on the definition of the link budget for the proposed scenario. The operation of a prototypal LoRa sensor node is then tested in a real scenario, analyzing the performances according to the different Spreading Factors (SF). Actual data transmission is achieved at a depth of 30 cm, thus suggesting the usage of such a technology for real time monitoring applications in environments, like swimming pools, rivers or fish farms.**

I. INTRODUCTION

The underwater environment represents a totally different application scenario if compared to the terrestrial one since significant physical characteristics of the aquatic medium impose strong limitations on the usable technologies. Salinity, temperature, pressure, density, conductivity, water-air interface, reflections, scattering, wave motions are just some of the variables that must be taken into account in the creation of an underwater communication channel. These constraints hindered the implementation of Underwater Wireless Sensor Networks (UWSNs), slowing their development in comparison with terrestrial Wireless Sensor Networks (WSNs). However, the UWSNs could find application in multiple activities, making them much more independent from human intervention than they currently are. Typical use cases can be: pipeline and off-shore oil and gas plants monitoring, navigation, coastal surveillance, environment protection, Autonomous Underwater Vehicles (AUVs) and Remotely Operated Vehicles (ROVs) management.

There are three main technologies employed so far in underwater wireless communication, each one with pros and cons [1–7]. Optical [4–6] and acoustic [7] communications are well-known technologies and the most used solutions in the implementation of underwater networks. Acoustic carriers can reach the higher propagation distance (in the order of kilometers) while optic waves have

a reduced range of 10-100 m because of rapid absorption, nevertheless they guarantee a high data rate up to Gbps. The main drawbacks of acoustic transmission are the severe sensitivity to several sources of ambient noise (bubbles, animals, obstacles, ships, etc) and the strong dependence on water properties as temperature, pressure and salinity: their sudden variations can cause discontinuities in the medium, responsible for wave reflections and absorptive energy losses during waves propagation. The usage of acoustic carriers is strongly advised solely in deep water since in shallow water the performances may be degraded by the several reflections induced by the bottom and the water surface, leading to multipath effect. As a consequence of the slow propagation speed of sound (typically 1500 m/s), the multipath reflections have high propagation delays and the resultant time dispersion brings to interferences that make unreadable the transmitted signal. Also, optic carriers are very susceptible on water composition, in particular purity, turbidity and presence of suspended particles that may originate optical scattering.

All these drawbacks can be overcome by electromagnetic transmission, whose performance is not affected by multipath, scattering, Doppler Effect, water depth, medium discontinuities, turbidity and waves movements. Furthermore, electromagnetic waves are able to cross water-air and water-seabed interfaces and have no well-known consequences on aquatic animals, in contrast to acoustic carriers. Moreover, an electromagnetic UWSN does not require tight alignment and line-of-sight constraint between transmitter and receiver, as optic transmission does. Despite all these advantages, the solution that involves the use of radio frequency carriers is the least used because electromagnetic propagation under water is strongly affected by the electric characteristics of the medium, leading to reduction in speed and severe attenuation. The correct operation is demonstrated only in a reduced range of frequencies, generally the Extremely Low Frequencies (ELF) and the Very Low Frequencies (VLF), since they experiment less attenuation and they achieve higher distances (up to several kilometres). However, working in these operating ranges implies very low data rates, high power and the adoption of antennas with size in the order of some meters, making

the design of dense and extensive sensor networks quite impractical.

To our knowledge, scientific works concerning underwater networks based on EM technology are primarily limited to ELF (3 Hz-3 kHz) and VLF (3 kHz-30 kHz) but, as stated before, these solutions are inapplicable to distributed sensor networks. Several studies focus on underwater electromagnetic transmission, analyzing the expected performances in terms of wavelength, signal strength and attenuation from few Hz to GHz, however the results obtained confirm that at High, Very High and Ultra High Frequencies (HF, VHF, UHF) it is substantially impossible to establish a reliable communication channel. The goal of our paper is to demonstrate the possibility to implement an underwater to air transmission at the frequency of 868 MHz using LoRa technology, thus opening possible scenarios for the design of distributed sensor networks. In particular, the performed transmission tests are limited to the fresh water case, with plausible future applications in the monitoring of pools, fountains, rivers and fish farming.

II. ELECTROMAGNETIC PROPAGATION IN WATER

Electromagnetic waves behave in different manner according to the type of water medium they are propagating through. In particular, the difficulty of propagation increases with the growth of the medium's conductivity. In this sense, seawater is a high-loss medium compared to fresh water because of the massive presence of dissolved substances, especially linked to salinity. The average value of conductivity σ for the sea water is 4 S/m, while the typical value for fresh water is 0.01 S/m. Concerning magnetic permeability, both sea and fresh water have the same permeability of air ($\mu = \mu_0\mu_r = 4\pi \times 10^{-7} \times 1 = 1.2566 \times 10^{-6}$ H/m), whilst the relative dielectric permittivity $\widetilde{\epsilon_r}$ of water has a complex form strongly correlated to salinity content and working frequency.

The physical laws ruling the underwater electromagnetic transmission can be thus summarized [8,9]. The propagation constant in a lossy medium is

$$\gamma = j\omega\sqrt{\widetilde{\epsilon}\mu} = j\omega\sqrt{\mu\epsilon - j\frac{\mu\sigma}{\omega}} =$$
$$= j\omega\sqrt{\mu\epsilon(1 - j\frac{\sigma}{\omega\epsilon})} = j\omega\sqrt{\mu\epsilon(1 - j\,tan\,(\theta))} =$$
$$= j\omega\sqrt{\mu\,(\epsilon' - j\epsilon'')} = \alpha + j\beta \quad (1)$$

considering the complex permittivity of the medium as

$$\widetilde{\epsilon} = \epsilon_0\widetilde{\epsilon_r} = \epsilon_0(\epsilon_r' - j\epsilon_r'') = \epsilon(1 - j\frac{\sigma}{\omega\epsilon}) =$$
$$= \epsilon - j\frac{\sigma}{\omega} = \epsilon' - j\epsilon'', \quad (2)$$

where the real part of the relative dielectric permittivity ϵ_r' is equal to 81 F/m and the imaginary part accounts for

loss in the medium. Another factor to take into account for losses is the loss tangent $tan\theta = \frac{\epsilon'}{\epsilon''} = \frac{\sigma}{\omega\epsilon}$. In particular,

$$\alpha = \omega\sqrt{\frac{\mu\epsilon}{2}\left(\sqrt{1 + \left(\frac{\sigma}{\omega\epsilon}\right)^2} - 1\right)} =$$
$$= \omega\sqrt{\frac{\mu\epsilon}{2}\left(\sqrt{1 + (tan\theta)^2} - 1\right)}\frac{Np}{m} \quad (3)$$

is the attenuation constant (taking into account the decay of the wave amplitude during its propagation) and

$$\beta = \omega\sqrt{\frac{\mu\epsilon}{2}\left(\sqrt{1 + \left(\frac{\sigma}{\omega\epsilon}\right)^2} + 1\right)} =$$
$$= \omega\sqrt{\frac{\mu\epsilon}{2}\left(\sqrt{1 + (tan\theta)^2} + 1\right)}\frac{rad}{s} \quad (4)$$

is the phase constant (concerning the wave oscillation); thus the propagating wave can be written as

$$\overrightarrow{E(z)} = E_0 e^{j\omega t - \gamma z} = E_0 e^{-\alpha z} e^{j(\omega t - \beta z)} . \quad (5)$$

The attenuation constant is linked to the skin depth $\delta = \frac{1}{\alpha}$, which gives a measure of how much the amplitude is attenuated during propagation: for each distance travelled by the wave and equals to δ, the wave amplitude is decreased by a factor e (8.7 dB).

The wavelength and the propagation velocity depend on β according to $\lambda = \frac{v_p}{f} = \frac{2\pi}{\beta}$ and $v_p = \frac{\omega}{\beta}$; the intrinsic impedance of the medium is the complex number computed as

$$\eta = \sqrt{\frac{j\omega\mu}{(j\omega\epsilon + \sigma)}} = \sqrt{\frac{\mu}{\epsilon(1 - j\tan\theta)}} \quad (6)$$

with modulus and phase

$$|\eta| = \sqrt{\frac{\frac{\mu}{\epsilon}}{\sqrt{1 + \left(\frac{\sigma}{\omega\epsilon}\right)^2}}} \quad \angle(\eta) = \frac{1}{2}tan^{-1}\frac{\sigma}{\omega\epsilon}. \quad (7)$$

Compared to fresh water, sea water is a good conductor, hence for operating frequencies lower than $\simeq 888$ MHz the condition $\sigma \gg \omega\epsilon$ is satisfied [3]; in this case

$$\alpha = \beta = \sqrt{\frac{\omega\mu\sigma}{2}} = \sqrt{\pi\,f\mu\sigma} \quad (8)$$

so the attenuation constant is frequency dependent and lower frequencies must be preferred in order to reduce attenuation. Moreover, $\eta = \sqrt{\frac{j\omega\mu}{\sigma}}$ and $\delta = \sqrt{\frac{2}{\omega\mu\sigma}} = \frac{1}{\sqrt{\pi f\mu\sigma}}$.

Instead, for frequencies greater than few MHz, fresh water behaves as a low-loss medium ($\sigma \ll \omega\epsilon$); hence approximately $\alpha \simeq \frac{\sigma}{2}\sqrt{\frac{\mu}{\epsilon}}$ and $\beta = \omega\sqrt{\epsilon\mu}$ so the attenuation constant is independent from frequency. Furthermore, $\eta = \sqrt{\frac{\mu}{\epsilon}}$, $\delta = \sqrt{\frac{4\epsilon}{\mu\sigma^2}}$, $v_p = \frac{1}{\sqrt{\epsilon\mu}} = \frac{c}{\sqrt{\epsilon'_r \mu_r}}$ and $\lambda = \frac{1}{f\sqrt{\epsilon\mu}}$. Therefore, it can be seen that the wave speed underwater is slowed down by a factor of $\sqrt{\epsilon'_r} = 9$ with respect to the vacuum, anyway channel spread issues are avoid since the actual velocity is sufficiently high.

III. THEORETICAL ANALYSIS

In the proposed scenario the tests are performed in fresh water so we can suppose $\sigma = 0.01$ S/m. The working frequency is 868 MHz, then the condition

$$\omega \gg \frac{\sigma}{\epsilon} \rightarrow f \gg \frac{\sigma}{2\pi\epsilon} \rightarrow 868 \times 10^6 \gg$$
$$\gg \frac{0.01}{2\pi \times 81 \times 8.854 \times 10^{-12}} = 2.219 \times 10^6 \frac{rad}{s} \quad (9)$$

is satisfied. This implies that the following formulas are valid:

$$\alpha = \frac{\sigma}{2}\sqrt{\frac{\mu}{\epsilon}} = \frac{0.01}{2}\sqrt{\frac{4\pi \times 10^{-7}}{81 \times 8.854 \times 10^{-12}}} = 0.209 \frac{N_p}{m} \quad (10)$$

$$\beta = \omega\sqrt{\epsilon\mu} =$$
$$= 2\pi \times 868 \times 10^6 \sqrt{81 \times 8.854 \times 10^{-12} \times 4\pi \times 10^{-7}} =$$
$$= 163.725 \frac{rad}{m} \quad (11)$$

$$\eta = \sqrt{\frac{4\pi \times 10^{-7}}{81 \times 8.854 \times 10^{-12}}} = 41.859\,\Omega \quad (12)$$

$$\delta = 4.784 \frac{m}{N_p} \quad (13)$$

$$v_p = \frac{1}{\sqrt{81 \times 8.854 \times 10^{-12} \times 4\pi \times 10^{-7}}} = 3.33 \times 10^7 \frac{m}{s} \quad (14)$$

$$\lambda = \frac{v_p}{f} = \frac{3.333 \times 10^7}{868 \times 10^6} = 0.038\,m. \quad (15)$$

The impedance mismatch between air ($\simeq 376.73\,\Omega$) and fresh water ($41.86\,\Omega$) determines reflections at the air-water interface; supposing normal incidence, the reflection and the transmission coefficients are computed as [10]

$$\Gamma = \frac{\eta_{air} - \eta_{water}}{\eta_{air} + \eta_{water}} \simeq 0.80 \quad (16)$$

$$T = \frac{2\eta_{air}}{\eta_{air} + \eta_{water}} \simeq 1.80. \quad (17)$$

The refractive index of the medium is equal to $n = \frac{c}{v_p}$, with c speed of light; $n_1 = \sqrt{\epsilon'_r} = 9$ and $n_2 = 1.0003$ are respectively the refractive indexes of water and air. Considering a transition from water to air, the critical angle for the incident wave above which the total internal reflection phenomenon happens can be derived from Snell's Law as $\psi_L = sin^{-1}\frac{n_2}{n_1} \simeq 6.38°$ [11]. Therefore, only the electromagnetic waves impinging on the air-water boundary with an incident angle lower that ψ_L can cross the interface and propagate through air. In our scenario the transmission is given by the lateral waves contribution; considering that they intersect the air-water boundary mostly above the underwater transmitter, it can be supposed that the incidence is approximately orthogonal (or for angles lower than ψ_L) and the total internal reflection effect should never happen.

A. Link Budget

In order to properly characterize the wireless channel, the link budget must be computed considering both transmission in water (from underwater node to water surface) and in air (from water surface to receiver node) [10–12]. Globally, $PL_{tot} = PL_{AW} + PL_{UW2AW} + PL_{UW} + L_M$. PL_{AW} is the free space path loss for the above water path, and can be described by the following equation:

$$PL_{AW} = L_0 = 20\log_{10}\frac{4\pi d_{AW}}{\lambda_0} =$$
$$= 20\log_{10} d_{AW} + 20\log_{10} f - 147.5 \quad (18)$$

where d_{AW} and $\lambda_0 = 0.3454\,m$ are respectively the travelled distance and the wavelength in free air. PL_{UW2AW} takes into account the losses due to the medium discontinuity at the water-air interface and is described by the following equation:

$$PL_{UW2AW} = 10\log_{10}(|T|^2 \, Re\{\frac{\eta_{water}}{\eta_{air}}\})^{-1} \quad (19)$$

with T the reflection coefficient obtained from eq. 17. Finally, PL_{UW} is the underwater path loss experienced by the lateral waves that accounts for the attenuation coefficient α and for the wavelength reduction because of the spreading through water; it is composed of three terms:

$$PL_{UW} = L_\beta + L_\alpha + L_W =$$
$$= 20\log_{10}\frac{\lambda_0}{\lambda_{UW}} + 10\log_{10} e^{2\alpha d_{UW}} + 20\log_{10}\frac{4\pi d_{UW}}{\lambda_0} =$$
$$= 8.69\alpha d_{UW} + 20\log_{10} d_{UW} + 20\log_{10}\beta + 6 \quad (20)$$

with d_{UW} depth of propagation inside water and $\lambda_{UW} = 0.0384\,m$ wavelength inside water. L_M is a term linked to miscellaneous losses due to possible sources (e.g., buildings, antennas polarization mismatch, beam defocusing and so on) and assumed equal zero in our model.

So, globally the received power P_r can be calculated as

$$P_r = P_t + G_r + G_t - PL_{tot} \qquad (21)$$

with P_t transmitted power (14 dBm), G_r receiving antenna gain (14 dBi for a directional helical antenna) and G_t transmitting antenna gain (1.2 dBi for $\lambda/4$ dipole).

The RSSI behaviour in function of the underwater node depth d_{UW} is shown in Figure 1: the link budget equation is computed assuming $f = 868$ MHz, $d_{AW} = 35$ m and deriving α, η, T, β from previous formulas.
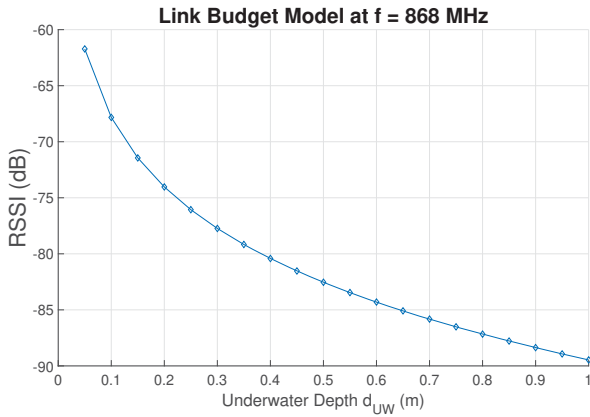

Fig. 1. *Link budget model for the UW2AW transmission computed according to equation 21 assuming $f = 868$ MHz and $d_{AW} = 35$ m.*
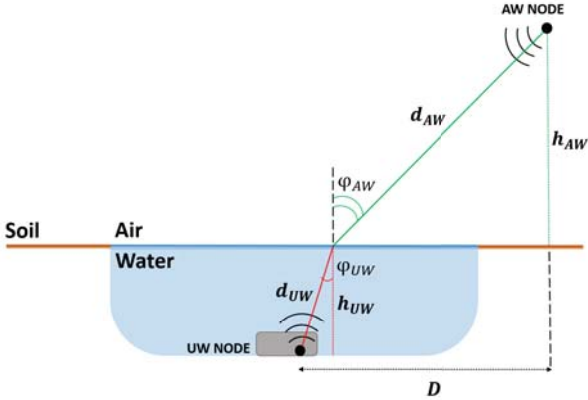

Fig. 2. *Geometric representation of the UW2AW link according to the test scenario.*

The operating scenario is simplified in the drawing of Figure 2. As stated in section III, the waves impinge on the air-water boundary in an roughly normal manner, therefore $\psi_{UW} \simeq 0$. As a consequence, the underwater distance d_{UW} can be approximated with the burial depth $\simeq h_{UW}$ and the path d_{AW} travelled in free space can be computed as $\sqrt{D^2 + h_{AW}^2}$.

IV. EXPERIMENTAL SETUP

In order to test the performances of the 868 MHz LoRa transmission underwater, an experimental setup based on a LoRa sensor node positioned inside a waterproof IP68 ABS plastic box has been developed. The sensor node is composed of a Microchip ATtiny84 microcontroller connected to a HopeRF RFM95x LoRa transceiver. Data is sampled from a LM35 temperature sensor and transmitted by means of LoRaWAN protocol to a LoRaWAN Gateway based on a RAKWireless RAK831 multi-channel concentrator connected to a Raspberry Pi B board. The sensor node is powered by means of two parallel 18650 Li-Ion batteries: the whole hardware is placed inside the plastic box, whose dimensions are roughly 24x12x8 cm.

The tests are performed in an outdoor circular fountain with diameter of 5 m and maximum depth of 30 cm. The receiver is located in the near building with the helical antenna in front of the window and turned toward the fountain direction; the transmitting node is held on the bottom of the fountain by means of stones used as ballast (see Figure 3).
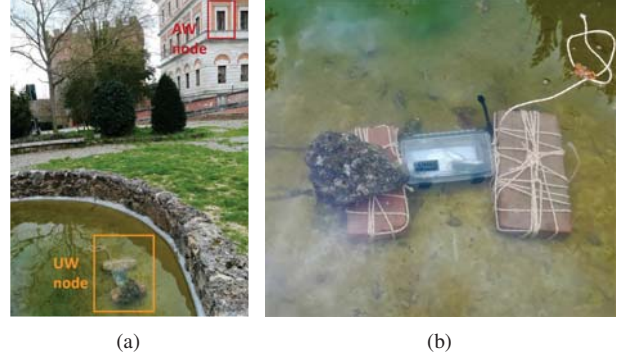

(a)   (b)

Fig. 3. *The test set-up: (a) operating scenario with the underwater node in the foreground (orange box) and the receiving LoRa node in the background building (red box), (b) transmitting LoRa node inside the waterproof box and held under 30 cm of water by means of stones as weights.*

V. TEST AND RESULTS

As explained in the previous section, the communication takes place from underwater to air hence the crossing of the electromagnetic wave at the air-water interface must be accounted. The underwater node is tested at a depth of 30 cm and changing the spreading factor (SF) of the transmitting LoRa module from 12 to 7; 550 packets are sent for each SF and the payload is constant and equal to 24 Bytes. In particular, RSSIs, SNRs and packet losses are collected and the obtained results are shown in Table 1.

It can be seen that the RSSI value is unaffected by the spreading factors variations and it is approximately 32 dBm lower than the theoretical result obtained from the

Table 1. Test results at an underwater depth of 30 cm and for SF = 12-7: means and standard deviations for RSSIs and SNRs values, packet losses.

SF	RSSI [dBm]		SNR [dB]		PL [%]
	μ_{RSSI}	σ_{RSSI}	μ_{SNR}	σ_{SNR}	
12	-109.26	2.46	-4.04	3.71	4.36
11	-109.66	2.07	-4.93	3.93	12.55
10	-109.88	2.05	-6.8	3.7	20
9	-110.54	1.82	-7.13	3.17	28.73
8	-110.05	1.81	-6.64	2.77	38.73
7	-109.12	1.53	-5.49	2.06	63.1

link budget model of equation 21 and depicted in Figure 1, from which a RSSI = -77.7 dBm at $d_{UW} = 30$ cm can be assessed. The factor causing the receiving power degradation might be the presence of miscellaneous losses not considered in the theoretical link budget model and caused by additional dispersive phenomena (e.g. presence of obstacles, building crossing etc). Probably, even the lack of knowledge of salinity and composition of the water used during the test may be an additional degradation reason.

Another important information inferred by the collected results is the packet loss, whose percentage increases with the decreasing of the spreading factor. This aspect is coherent with the LoRa [13] protocol according to which an higher SF implies a longer time on air, a greater sensitivity and consequently a better coverage; therefore the SF = 12 is the optimal choice.

The negative SNR values collected highlight the fact that LoRa technology is capable of correctly demodulating the received signal even in presence of very noisy channels.

Figures 4-7 respectively show the RSSI and the SNR trend during the experiment and the RSSI and the SNR Probability Mass Function (PMF), for each SF from 12 to 7.

VI. CONCLUSIONS

The aim of this paper was to demonstrate the feasibility of a LoRa radio link for the transmission of data packets from an underwater sensor node to an above water Gateway in charge of receiving them and storing them in a Cloud infrastructure. The theoretical analysis, suggesting the feasibility of this connection, was demonstrated by a set of preliminary tests carried out in a real application scenario.

Following this first set of tests, further work is expected to be carried out in two different directions. First of all, test concerning the maximum achievable transmission depth are planned: these tests are expected to be carried out in a swimming pool, whose depth is around 2 m and, in case of positive output, in a lake, whose depth is even larger. The second direction foresees the test of the system in marine water: in this case, the theoretical analysis suggests an increased level of complexity that makes the realization of
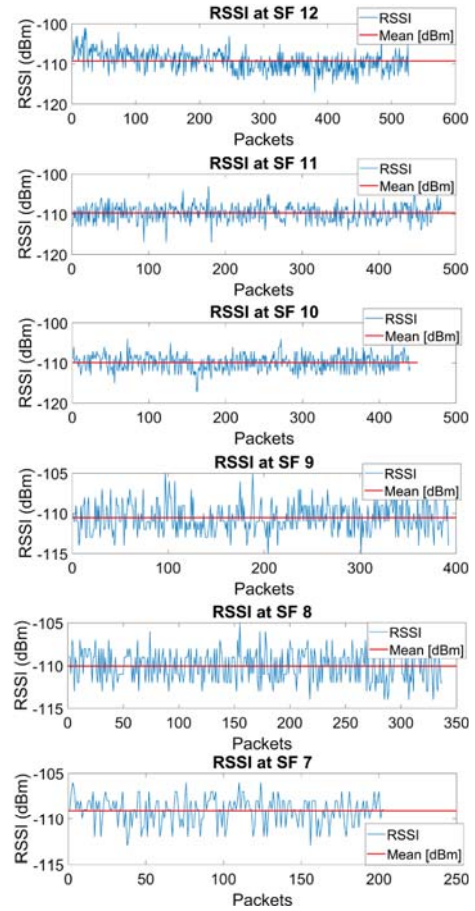

Fig. 4. RSSI trend at different spreading factor from SF = 12 to SF = 7.

an efficient radio channel even more challenging.

REFERENCES

[1] M. F. Ali, D. N. K. Jayakody, Y. A. Chursin, S. Affes, S. Dmitry, "Recent Advances and Future Directions on Underwater Wireless Communications", Archives of Computational Methods in Engineering, 2019, pp. 1-34.

[2] C. M. Gussen, P. S. Diniz, M. L. Campos, W. A. Martins, F. M. Costa, J. N. Gois "A survey of underwater wireless communication technologies", J. Commun. Inf. Sys., 2016, 31(1), pp. 242-255.

[3] L. Lanbo, Z. Shengli, C. Jun-Hong. "Prospects and problems of wireless communication for underwater sensor networks", Wireless Communications and Mobile Computing, 2008, 8(8), pp. 977-994.

[4] N. Saeed, A. Celik, T. Y. Al-Naffouri, M. S. Alouini, "Underwater optical wireless communications, networking, and localization: A survey", Ad Hoc Networks, 2019, 94, 101935.
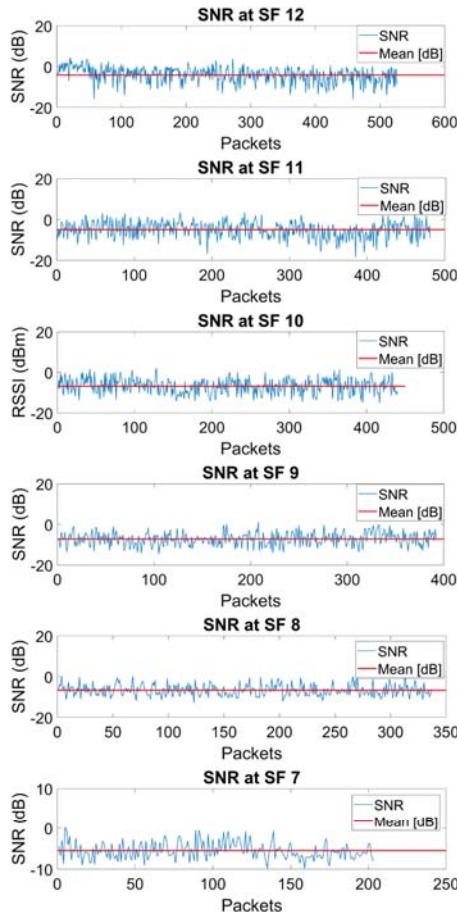
[5] H. Kaushal, G. Kaddoum, "Underwater optical wire-

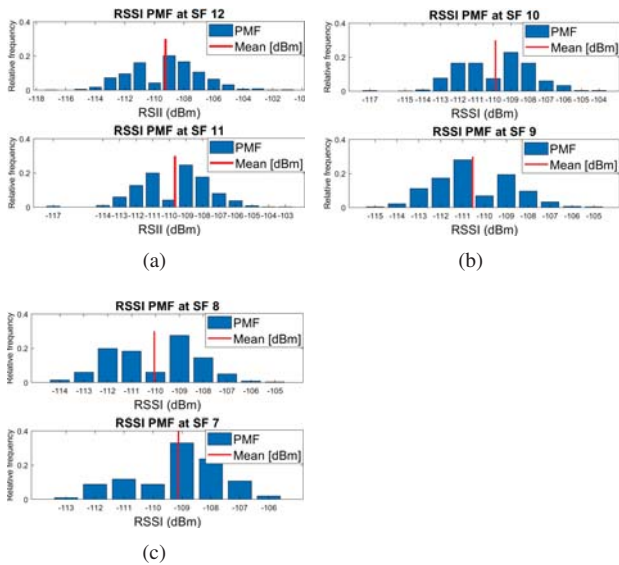*Fig. 5. SNR trend at different spreading factor from SF = 12 to SF = 7.*

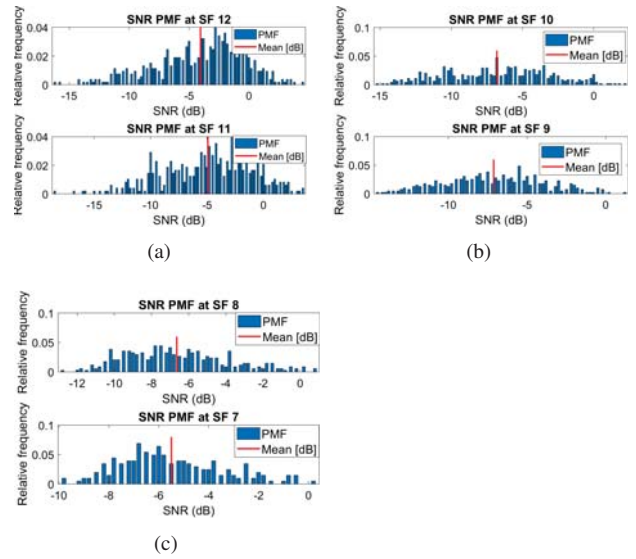*Fig. 6. RSSI PMF and mean value at different spreading factor from SF = 12 to SF = 7.*

Fig. 7. SNR PMF and mean value at different spreading factor from SF = 12 to SF = 7.

less communication", IEEE access, 2016, 4, pp. 1518-1547.

[6] Z. Zeng, S. Fu, H. Zhang, Y. Dong, J. Cheng, "A survey of underwater optical wireless communications", IEEE communications surveys & tutorials, 2016, 19(1), pp. 204-238.

[7] M. Murad, A. A. Sheikh, M. A. Manzoor, E. Felemban, S. Qaisar, S, "A survey on current underwater acoustic sensor network applications", International Journal of Computer Theory and Engineering, 2015, 7(1), 51.

[8] M. N. Sadiku, "Elements of electromagnetics", Oxford university press, 2014.

[9] J. S. Seybold, "Introduction to RF propagation", John Wiley & Sons, 2005.

[10] G. Hattab, M. El-Tarhuni, M. Al-Ali, T. Joudeh, N. Qaddoumi, "An underwater wireless sensor network with realistic radio frequency path loss model", International journal of distributed sensor networks, 2013, 9(3), 508708.

[11] K. P. Hunt, J. J. Niemeier, A. Kruger, "RF communications in underwater wireless sensor networks", In 2010 IEEE International Conference on Electro/Information Technology, May 2010, pp. 1-6.

[12] Z. H. I. Sun, I. F. Akyildiz, G. P. Hancke, "Dynamic connectivity in wireless underground sensor networks", IEEE Transactions on Wireless Communications, 2011, 10(12), pp. 4334-4344.

[13] Semtech, "SX1272/3/6/7/8: LoRa Modem Designer's Guide AN1200.13", Semtech Corporation, 2013.